Proceedings of the 17th World Congress
The International Federation of Automatic Control
Seoul, Korea, July 6-11, 2008

Passive P-Control of a Grid-Connected Photovoltaic Inverter ⋆

Carlos Meza * **Dimitri Jeltsema** ** **Jacquelien Scherpen** ***
Domingo Biel *

* *Institut of Industrial and Control Engineering, UPC, Barcelona, Spain (e-mail: carlos.meza@upc.edu)*
** *Delft Institute of Applied Mathematics, Delft University of Technology, The Netherlands (e-mail: d.jeltsema@tudelft.nl)*
*** *Faculty of Mathematics and Natural Sciences, ITM, University of Groningen, The Netherlands(e-mail:j.m.a.scherpen@rug.nl)*

Abstract: A passive P-controller for a single-phase single-stage grid-connected photovoltaic inverter is presented. Explicit dependance of the PV array parameters on external unpredictable variables such as temperature and solar irradiance is avoided by extending the control scheme with a reference estimator. A detailed simulation study shows the closed-loop behavior meets the desired control objectives.

Keywords: Nonlinear systems, solar energy, power circuits, inverters, power generation.

1. INTRODUCTION

Photovoltaic (PV) energy generation represents a renewable energy alternative that is becoming more competitive due to the new favorable governmental laws and policies as recently introduced. Due to their portability (solar irradiance is found almost anywhere) PV systems have been first used as stand-alone systems in remote areas where utility lines are not available or are uneconomical to install. Since solar energy is not available all day a battery subsystem is needed in order to make the electricity available whenever is required. The major drawback of stand-alone PV systems is that the battery is a costly and bulky element that needs to be properly sized in order to obtain maximum efficiency from the PV system. Stand-alone PV systems do not always extract the maximum amount of energy from the PV cells and are only economically justifiable in some remote locations where other sources of energy are not available.

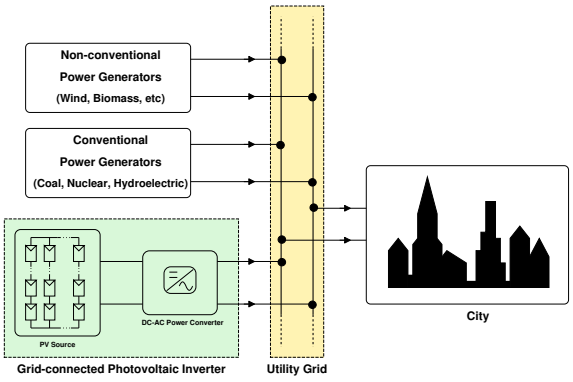

Fig. 1. Grid-connected Photovoltaic System block diagram

Another possibility to take advantage of a PV system is feeding the generated PV energy directly into the utility grid system. In most parts of the industrially developed world grid electricity is easily accessible and can be used as a giant "battery" to store all the energy produced by the PV cells. The grid can absorb PV power that is surplus to current needs, making it available for use by other customers and reducing the amount of energy that has to be generated by conventional means. At night or on cloudy days, when the output of the PV system is insufficient to the energy needs, the grid will provide the backup energy from conventional sources. Removing the battery subsystem not only represents a considerable cost and size reduction of the whole system but also increases its reliability: while a PV panel lasts more than twenty years a battery operates for at most five years and need periodic maintenance (Cruz-Martins and Demonti [2001]).

Figure 1 shows the basic structure of a grid-connected PV system. The main components include a series-parallel connection arrangement of the available PV panels and a power conditioning system that regulates the power transfer from the PV panels to the grid. A control strategy for the power conditioning system has to be designed in order to extract and to properly transfer the maximum available power from the PV panels to the grid. In the reviewed literature few words have been said about the control scheme for grid-connected PV inverters. To our knowledge, the majority of articles seem to focus only on the design of novel power inverter architectures and present neither a well defined methodology to design the inverter's controllers nor a rigorous stability analysis. A main difficulty in analyzing the stability of the closed-loop system is the inherently nonlinear time-vayring electrical characteristics of the grid-connected photovoltaic inverter and its dependance on unpredictable environmental conditions such as temperature and solar irradiance.

In this paper, a passive controller that considers the nonlinear time-varying dynamics of the system and assures global stability under certain known conditions is designed for a single-

⋆ This work has been partially sponsored by the Ministerio de Ciencia y Tecnología, España, DPI2006-15627-C03-01, DPI2007-62582 by the European Union (FEDER)

phase single-stage grid-connected photovoltaic system. These known conditions comprise the exact knowledge of the PV array model parameters. For the case in which the PV array model is unknown the passive control scheme is modified adding a reference estimator and its appropriate closed-loop behavior is validated by means of a detailed simulation study.

2. GRID-CONNECTED PV SYSTEM UNDER STUDY

As discussed in the previous section, a grid-connected PV system consists of a series-parallel connection array of PV panels connected to a power conditioning system stage (also referred to as grid-connected PV inverter, or in short GPV inverter) which is responsible for the proper transfer of the energy produced by the PV array to the grid (see also Figure 1). This section briefly describes each subsystem and introduces the mathematical models used for analysis, controller design, and controller validation.

2.1 Photovoltaic Array

The PV cell is the basic building block of a PV system in which the photovoltaic effect occurs. The electrical behavior of a photovoltaic cell is highly nonlinear and exhibits maximum power point characteristics. A PV panel is defined as the largest unit combination of PV cells that is mechanically designed to facilitate manufacture and handling and that establishes a basis for electrical performance test (IEEE [1969]). A single typical commercial PV panel generates a maximum of 110 W with a voltage between $15-24$ V when an incident irradiance of 1000 Wm^{-2} is present. Usually a number of PV panels are electrically connected to form one or more arrays. The number of elements of each array varies depending on the overall system's requirements.

Solar cells share many of the same processing and manufacturing techniques of other semiconductor devices. However, the stringent requirements for cleanliness and quality control of semiconductor fabrication are a little more relaxed for solar cells. Most large-scale commercial solar cell factories today make screen printed poly-crystalline silicon solar cells. Single crystalline wafers which are used in the semiconductor industry can be made into excellent high efficiency solar cells, but they are generally considered to be too expensive for large-scale mass production. The current solar cell manufacturing process does not allow to obtain PV panels conformed with identical PV cells, this makes it very difficult to identify its parameters without measuring each single cell. It is important to take into account that a GPV system not only inherently presents model uncertainties associated to its fabrication process but also depends on unpredictable and difficult to measure external variables such as the solar incident irradiance.

In order to exemplify the electrical behavior of a PV cell a simple solar cell model is presented. This model was introduced by Prince [1955] and represents the PV cell as an ideal p-n junction with a constant current source in parallel with the junction as depicted in Figure 2. More complete PV cell models can be found in Gow and Manning [1999], Liu and Dougal [2002].

The current source $I_{\mathrm{g_{cell}}}$ represents the light-induced current and the current flowing through the diode can be derived from the equations of an ideal pn-junction:

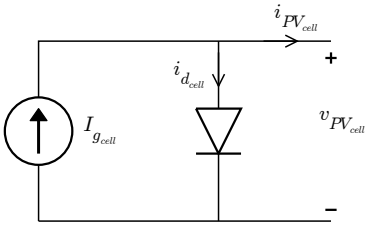

Fig. 2. PV Cell Ideal Model.

$$i_{\mathrm{d_{cell}}} = I_{\mathrm{sat_{cell}}}\left[\exp\left(\frac{v_{\mathrm{PV_{cell}}}}{\eta v_{T_{\mathrm{cell}}}}\right)-1\right], \tag{1}$$

where η is the emission coefficient which varies between 1 and 2 depending on the fabrication process and semiconductor material, $I_{\mathrm{sat_{cell}}}$ is the reverse saturation current of the pn-junction and $v_{T_{\mathrm{cell}}}$ is the thermal voltage defined as

$$v_{T_{\mathrm{cell}}} = \frac{k_B T}{e}. \tag{2}$$

Here, k_B and e are the Boltzmann constant and the electron's charge, respectively and T represents the cell's temperature. Based on the previous equations, a single exponential equation can be derived for the PV cell as follows:

$$i_{\mathrm{PV_{cell}}} = I_{\mathrm{g_{cell}}} - I_{\mathrm{sat_{cell}}}\left[\exp\left(\frac{v_{\mathrm{PV_{cell}}}}{\eta v_{\mathrm{T_{cell}}}}\right)-1\right]. \tag{3}$$

Figures 3 and 4 show the constitutive curves of a PV cell defined by the latter equations for different values of temperature and solar incident irradiance. Notice that there is a different maximum power point for each curve. Thus, during one day the maximum power point of a PV cell will vary accordingly to the solar incident irradiance and temperature changes.

The PV cell model can be extended to a PV array assuming that the PV array is formed by a set of series-parallel interconnected PV panels with identical PV cells operating under the same conditions. Accordingly the photovoltaic generator can be modeled by means of a function $f_{\mathrm{PV}} : \mathbb{U} \to \mathbb{I}$, where the instantaneous voltage and current of the photovoltaic array are denoted by $v_{\mathrm{PV}} \in \mathbb{U}$ and $i_{\mathrm{PV}} \in \mathbb{I}$ respectively. It is assumed that $\mathbb{U}, \mathbb{I} \subset \mathbb{R}^+$ and therefore the output power of the photovoltaic generator can only be positive. More specifically, function $f_{\mathrm{PV}}(v_{\mathrm{PV}}) = i_{\mathrm{PV}}$ is defined in the following way:

$$f_{\mathrm{PV}}(v_{\mathrm{PV}}) = \Lambda - \rho(v_{\mathrm{PV}}), \tag{4}$$

where $\Lambda \geq 0$ represents the part of the photovoltaic generator current that only depends on external variables (e.g., the solar irradiance). The last term of (4) denotes the direct link between the voltage of the photovoltaic generator and its current, i.e.,

$$\rho(v_{\mathrm{PV}}) = \Psi \exp(\alpha v_{\mathrm{PV}}), \tag{5}$$

where Ψ and α represent non-negative parameters of the photovoltaic generator. Referring to the equation of the PV cell (3), the parameters Λ, Ψ and α can be defined in the following way:

$$\begin{aligned}\Lambda &= (I_{\mathrm{g_{cell}}} + I_{\mathrm{sat_{cell}}})n_p,\\ \Psi &= I_{\mathrm{sat_{cell}}}\, n_p,\\ \alpha &= \frac{n_s}{\eta v_{T_{\mathrm{cell}}}},\end{aligned}$$

where n_s and n_p are the number of PV panels connected in series and parallel, respectively.

2.2 Power Conditioning System

Injecting PV energy into the grid introduces some practical problems. First of all, a solar array produces dc power which must be converted into ac before it can be injected into the grid. Secondly, the power conditioning system linking the solar array with the utility grid needs to facilitate an efficient energy transfer between them. This implies that the power stage has to be able to extract the maximum amount of energy from the PV array and it must assure that the output current presents low harmonic distortion, output unity power factor, and robustness to disturbances.

One of the most used GPV configurations is the so called "Central Inverter". In such configuration many PV panels are collected into one group and connected to the grid through a single power inverter (usually a full-bridge inverter). The PV array is consisting of a sufficient number of panels connected in series and parallel in order to reach the required power and voltage levels. In this way the system costs are considerably reduced since only one power conditioning module is needed. Additionally, a Central Inverter configuration requires a minimum of passive filter elements. Due to its extensive use and the possibility to easily add other power converter stages this has been chosen as the power conditioning structure considered in the present paper.

The schematic diagram of the full-bridge Central Inverter configuration is shown Figure 5. Here x_1 and x_2 are the actual input capacitor voltage and the output inductor current, respectively. Furthermore, as concluded from (3), the current i_{PV} generated by the PV array strongly depends on the incident solar irradiance, the temperature, and the input capacitor voltage. The utility grid voltage v_g is assumed to be sinusoidal with a constant amplitude A and a constant frequency ω, i.e., $v_g = A\sin(\omega t)$. The full-bridge inverter consists of four controllable switches, denoted by $u_1,\ldots,u_4$, taking values in the discrete set $\{0,1\}$ (i.e., OFF or ON, respectively). The switch control signals are generated via a pulse-width modulation (PWM) scheme with an input signal $\mu \in [-1,1]$ generated by the controller. This means that if the switching frequency is sufficiently high, the dynamical behavior of the GPV system can be approximated by the following set of differential equations

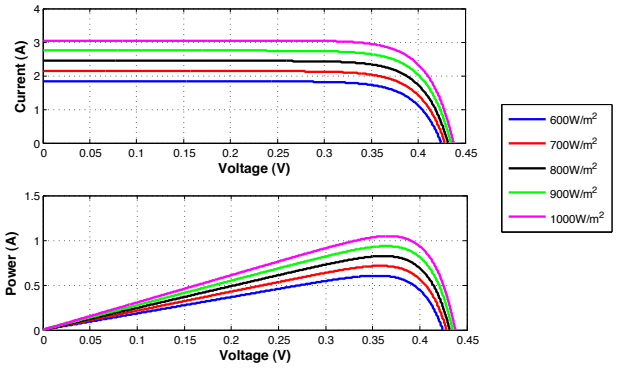

Fig. 3. PV Cell Electrical Curves with constant temperature and variable irradiance.

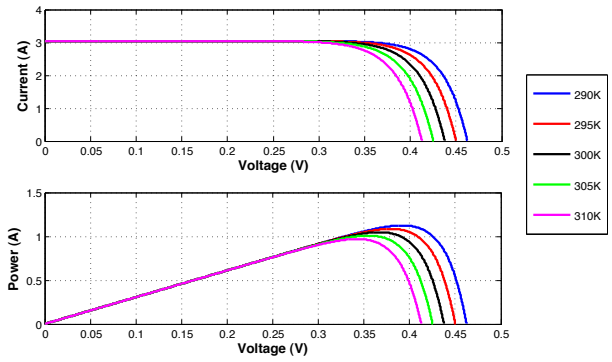

Fig. 4. PV Cell Electrical Curves with constant irradiance and variable temperature.

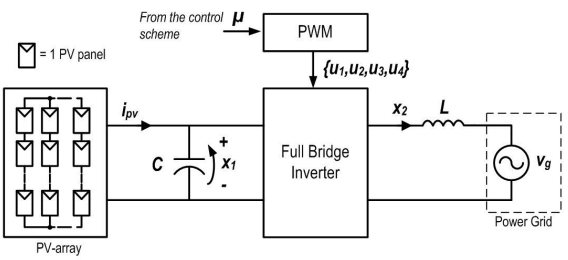

Fig. 5. Single-phase Single-stage GPV Inverter.

$$\begin{aligned} C\dot{z}_1 &= -\mu z_2 + \Lambda - \rho(z_1) \\ L\dot{z}_2 &= \mu z_1 - v_g, \end{aligned} \tag{6}$$

where z_1 and z_2 are the average values of x_1 and x_2, respectively. These equations will be used to design a controller for the system as discussed in the next section.

3. PROPOSED CONTROLLER

The main control objectives are as follows: the grid-connected PV system should

- C1. deliver a sinusoidal current in phase with the utility voltage of the power grid;
- C2. extract the maximum amount of power from the PV source.

Before we present our main result let us briefly review some existing approaches first.

3.1 Typical control scheme

In case of a single-phase single-stage PV inverter, like the one shown in Figure 5, the most common control scheme found in the literature (e.g., Meza et al. [2005], Casadei et al. [2006], and Kim et al. [2006]) is composed of two loops: an inner current control loop that determines the duty ratio for the generation of a sinusoidal output current, and an outer loop that determines the output power according to the maximum power point (MPP) of the PV array (see Figure 6). The latter loop operates on a much lower speed compared to the inner current control loop. Even though all the GPV systems that use this control scheme present good results in the simulations and/or in experimental tests, no rigorous proof of the stability of the closed-loop system have been found. In the next subsections a linear passive controller that renders the closed-loop system globally stable is presented.

3.2 Passive controller: PV array model known

Following Sanders and Verghese [1992], we start by decomposing the state variables z_i, with $i = 1,2$, into a steady-state part

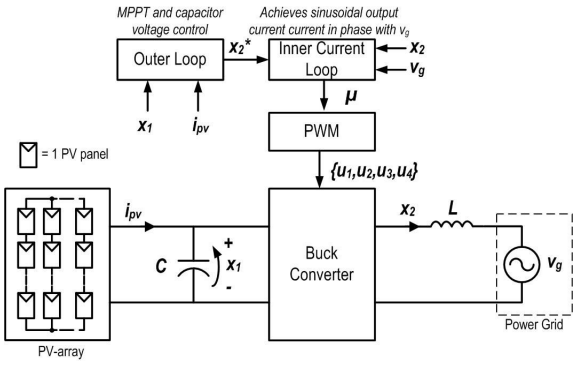

Fig. 6. Typical control scheme for the single-phase single-stage GPV inverter.

z_i^* and a dynamical part $\tilde{z}_i$, i.e., $z_i = z_i^* + \tilde{z}_i$. Similarly, the duty ratio function μ is decomposed into $\mu = \mu^* + \tilde{\mu}$. In this way, the system (6) can be rewritten as

$$\begin{aligned} C\big(\dot{\tilde{z}}_1 + \dot{z}_1^*\big) &= -\big(\tilde{\mu}+\mu^*\big)\big(\tilde{z}_2 + z_2^*\big) + \Lambda - \rho(z_1^*) - \tilde{\rho}(\tilde{z}_1, z_1^*) \\ L\big(\dot{\tilde{z}}_2 + \dot{z}_2^*\big) &= \big(\tilde{\mu}+\mu^*\big)\big(\tilde{z}_1 + z_1^*\big) - v_{\rm g}, \end{aligned}$$

where it is observed that $\rho(z_1)$ can be decomposed into

$$\rho(z_1) = \rho(z_1^*) + \tilde{\rho}(\tilde{z}_1, z_1^*),$$

with

$$\tilde{\rho}(\tilde{z}_1, z_1^*) = \Psi\left[\exp(\alpha\tilde{z}_1 + \alpha z_1^*) - \exp(\alpha z_1^*)\right].$$

Extracting the steady-state relations

$$\begin{aligned} C\dot{z}_1^* &= -\mu^* z_2^* + \Lambda - \rho(z_1^*) \\ L\dot{z}_2^* &= \mu^* z_1^* - v_g, \end{aligned} \tag{7}$$

leaves the input-nonlinear time-varying dynamical system

$$\begin{aligned} C\dot{\tilde{z}}_1 &= -\mu^* \tilde{z}_2 - \big(\tilde{z}_2 + z_2^*\big)\tilde{\mu} - \tilde{\rho}(\tilde{z}_1, z_1^*) \\ L\dot{\tilde{z}}_2 &= \mu^* \tilde{z}_1 + \big(\tilde{z}_1 + z_1^*\big)\tilde{\mu}, \end{aligned} \tag{8}$$

The key observation now is to associate with the latter system an energy-like function of the form

$$H(\tilde{z}_1, \tilde{z}_2) = \frac{1}{2}C\tilde{z}_1^2 + \frac{1}{2}L\tilde{z}_2^2. \tag{9}$$

Indeed, taking the time-derivative of H along the trajectories of (8) yields

$$\dot{H}(\tilde{z}_1, \tilde{z}_2) = \tilde{\mu}\left(z_1^*\tilde{z}_2 - z_2^*\tilde{z}_1\right) - \tilde{z}_1\tilde{\rho}\big(\tilde{z}_1, z_1^*\big). \tag{10}$$

Notice that the product $\tilde{z}_1\tilde{\rho}\big(\tilde{z}_1, z_1^*\big)$ is always positive given that function $\rho(\cdot)$ is strictly increasing, i.e., the function $\tilde{\rho}(\tilde{z}_1, z_1^*)$ is positive when $\tilde{z}_1 = z_1 - z_1^* > 0$ and negative when $\tilde{z}_1 < 0$. The latter directly suggests that the system is passive with respect to the supply rate $\tilde{\mu}\tilde{y}$, with $\tilde{y} = z_1^*\tilde{z}_2 - z_2^*\tilde{z}_1$, and positive definite storage function (9). This passivity statement (10) is very useful for control since it is easily translated into a Lyapunov stability argument by selecting a linear static proportional (P) feedback law

$$\tilde{\mu} = -K\tilde{y}, \tag{11}$$

with K an arbitrary non-negative constant. Hence, the system becomes strictly output passive, i.e.,

$$\dot{H}(\tilde{z}_1, \tilde{z}_2) = -K\tilde{y}^2 - \tilde{z}_1\tilde{\rho}\big(\tilde{z}_1, z_1^*\big) \leq 0, \tag{12}$$

for all $\tilde{z}_1, \tilde{z}_2$, which, together with the fact that (9) is a radially unbounded function, implies the closed-loop system is globally stable. However, to proof that the system is globally asymptotically stable we need to show that the only solution that keeps $\tilde{y} \equiv 0$ is the trivial solution $(\tilde{z}_1, \tilde{z}_2) = (0,0)$. In our case this is tantamount to showing that the system (8) is (zero-state) observable, which is easily asserted by calculating its time-varying observability matrix and applying Theorem 9.4 of Rugh [1995].

However, the main disadvantage of this control scheme is that precise knowledge of z_1^* and z_2^* is required. On the other hand, by considering (7) and invoking Tellegen's theorem, it is easily seen that z_1^* and z_2^* are related through the following "power-balance" relation

$$C\dot{z}_1^* z_1^* = z_1^*\left(\Lambda - \rho(z_1^*)\right) - L\dot{z}_2^* z_2^* - z_2^* v_g. \tag{13}$$

Solving the latter is very difficult because $\rho(z_1^*)$ is a nonlinear function depending not only on z_1^* but also on on the temperature, the incident irradiance, and the fabrication process of the PV arrays solar cells (see section 2). This problem can avoided as will be illustrated next.

3.3 Reference estimator: PV array model unknown

The main requirement for the single-phase single-stage GPV is output current injection at unity power factor, this means steady state output current proportional to the grid voltage, i.e.,

$$z_2^* = kv_g = kA\sin(\omega t), \tag{14}$$

whereas kA is the amplitude of the output current. We choose k to be time-varying to deal with varying input power (in order to be at the maximum power point), i.e., given that the output root mean squared power is proportional to k,

$$\langle P_{\rm out}\rangle_{\rm rms} = 0.5kA^2,$$

and that in steady state without losses $P_{\rm out} = P_{\rm in}$, the only way there is to adjust the input power is changing k. Since the current reference amplitude must maintain constant during a grid period (T_g) in order to reduce the output total harmonic distortion (THD) and to keep a unity power factor it has to be updated at grid cycles multiples. Since weather variations are slow, the input power will vary significantly slower than the dynamics of the power converter.

Taking into account the aforementioned requirement and defining $\bar{z}_1^*$ as the dc value of the output capacitor voltage in one grid cycle T_g, the control objective C1 can be redefined as follows: given $\bar{z}_1^*$, find $k(t) > 0$ such that (14) fulfills (13).

We proceed as follows. Equation (13) is rewritten as

$$\dot{E}_{\rm sto} = P_{\rm PV} - L\dot{z}_2^* z_2^* - v_g z_2^*, \tag{15}$$

where $E_{\rm sto} = \frac{1}{2}C(z_1^*)^2$ is the steady-state energy stored in the capacitor and $P_{\rm PV} = i_{\rm PV}z_1^*$ is the measured input power. Substituting $z_2^* = kv_g$, and integrating (15) over one grid cycle T_g yields the following energy-balance:

$$E_{\rm sto}(nT_g) - E_{\rm sto}((n-1)T_g) = E_{\rm PV} - \frac{1}{2}k((n-1)T_g)A^2T_g, \tag{16}$$

where $k((n-1)T_g)$ is the value of k at time $(n-1)T_g$, and

$$E_{\rm PV}(nT_g) = \int_{(n-1)T_g}^{nT_g} P_{\rm PV}(\tau)d\tau.$$

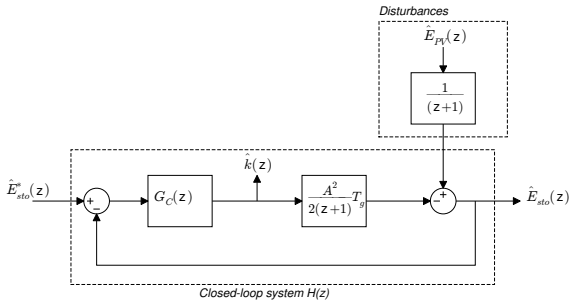

Fig. 7. Block diagram of the reference estimator.

Applying a Z-transform to the difference equation (16) yields

$$\hat{E}_{\text{sto}}(z) = Z\{E_{\text{PV}}\}\frac{z}{z-1} - \frac{\hat{k}(z)}{2(z-1)}A^2T_g. \tag{17}$$

If equation (17) is interpreted as an open-loop system for which the sampled value of E_{sto} has to be regulated to a desired value E^*_{sto}, one can close the loop by means of a linear controller G_C as is shown in Figure 7.

Note that, given an averaged reference value for z_1^*, the system of Figure 7 will converge to the correspondence value z_2^* that fulfills (13). Using the measurements of z_1 (sampled in one grid cycle) and using the value of k as the reference signal for the output current z_1^*, this value will eventually converge to the one that solves (13) for a given $\bar{z}_1^*$. The previous described subsystem will be referred to as the "reference estimator".

3.4 The Overall Control Scheme

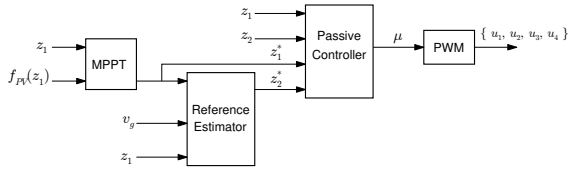

Fig. 8. Block diagram of the proposed controller.

The overall control scheme for the single-phase single-stage GPV system is summarized in Figure 8. It consists of three subsystems: the passive P-controller derived in subsection 3.2, the reference estimator just described, and a maximum power point tracking (MPPT) algorithm. The MPPT algorithm follows the same principle as the one described in Hua et al. [1998]. Here the capacitor voltage reference value is varied slowly (in the order of seconds) according to the variations of the measured input power. The reference value given by the MPPT algorithm is used by the reference estimator to generate the references that the P-passive controller requires. In the next section, the proposed control scheme is validated in a simulation experiment where the system is subject to abrupt solar irradiance changes.

4. SIMULATION RESULTS

In order to validate the presented control schemes the controlled system was tested using Matlab-Simulink. The parameters of the full-bridge power inverter were set to $L = 2$ mH and $C = 2.2$ mF. A PV array with identical elements that provides up to 2414 W when a solar irradiance of 1000 Wm^{-2} is used. The utility grid was assumed to be a purely sinusoidal source with an amplitude of 312 V and a frequency of 50 Hz. The reference estimator controller G_C (see Figure 7) is given by $G_C = 0.0012\frac{1-1.2z}{z-1}$, which is designed using the pole-placement technique in order to obtain a zero steady-state error (see Meza et al. [2005]).

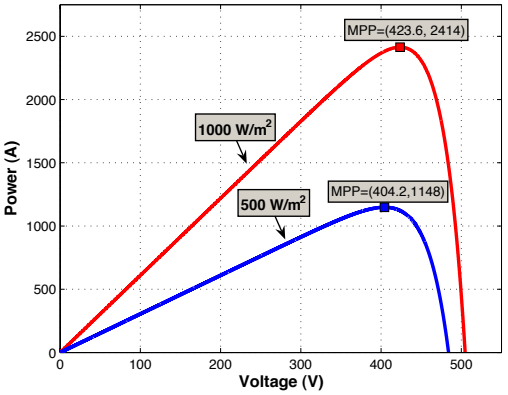

Fig. 9. Power vs. voltage curves of the PV array simulated with two different solar irradiances of 500 Wm^{-2} and 1000 Wm^{-2}.

The simulation test consisted of an abrupt solar irradiance change at $t = 4$ s from 1000 Wm^{-2} to 500 Wm^{-2}, which corresponds to the worst case scenario (e.g. sudden shadowing cause by a big cloud). The PV array power curves for both irradiances are shown in Figure 9. The test was performed for the passive P-controller with and without the reference estimator. In the case of the passive P-controller without the reference estimator the exact model of the PV array was used in order to obtain the reference signals. In both controllers the same MPPT algorithm (see Hua et al. [1998]) was used with an updating frequency of 0.1 s and a voltage variation of 0.25 V.

The simulation results are shown in Figures 10 to 13. It is seen that both control schemes achieve the control objectives C1 and C2. However, it is important to mention that the system with the P-controller without the reference estimator needs to use the exact model of the PV array in order to obtain both reference signals. On the other hand, the P-controller with the reference estimator also achieves a satisfactory behavior but without the need to know the exact model of the PV array. Referring to Figures 10 and 12, the value of the settling time after the power change is mainly due to the MPPT algorithm in both cases. Note that the closed loop system of the controller with reference estimator in Figure 13 needs one more grid cycle to converge to the desired output current amplitude in comparison with Figure 11.

5. FINAL REMARKS AND OUTLOOK

A passive P-controller for a single-phase single-stage grid-connected photovoltaic inverter that assures the global stability of the closed-loop system has been presented. The explicit dependance on the PV array parameters has been avoided by extending the control scheme with a reference estimator. The simulation study shows that the addition of the reference estimator does not affect the desired behavior of the closed-loop system. Nevertheless, the global stability of the augmented control scheme, i.e., with the reference estimator, has not been proved. We are currently extending the theoretical analysis considering the passive control with the reference estimator.

In order to validate the proposed control scheme under more realistic situations a laboratory prototype similar to the simulated example is being implemented. Moreover, the possibility of adding an integral action without affecting the stability of the system is under study. The addition of an integral action in the control scheme will make the system more robust against unmodeled elements of the inverter and the utility grid (voltage fluctuations, inductance variations, cable resistance, etc.). Additionally, the possibility to extend the proposed control scheme to other power converter configurations will be analyzed. Other grid-connected PV inverters configurations, possibly including solar irradiance sensors, can assure a more efficient energy extraction from the available PV panels—with the disadvantage of increasing the power processor's costs. Eventually, we would like to study the trade-off between the power processor's cost and the energy extraction efficiency taking into account different GPV inverter configurations.

REFERENCES

D. Casadei, G. Grandi, and C. Rossi. Single-phase single-stage photovoltaic generation system based on a ripple correlation control maximum power point tracking. *IEEE Transactions on Energy Conversion*, 21(2):562–568, June 2006.

D. Cruz-Martins and R. Demonti. Photovoltaic energy processing for utility connected system. In *The 27th Annual Conferences of the IEEE Industrial Electronics Society*, 2001.

J.A. Gow and C.D. Manning. Development of a photovoltaic array model for use in power-electronics simulation studies. *IEE Proc.-Electr Power Appl.*, 146(2):193–199, March 1999.

C. Hua, J. Lin, and C. Shen. Implementation of a dsp-controlled photovoltaic system with peak power tracking. *IEEE Transactions on Industrial Electronics*, 45(1):99–107, February 1998.

IEEE, editor. *IEEE Standard Definitions of Solar Cell*, November 1969.

Il-Song Kim, Myung-Bok Kim, and Myung-Joong Youn. New maximum power point tracker using sliding-mode observer for estimation of solar array current in the grid-connected photovoltaic system. *IEEE Transactions on Industrial Electronics*, 53(4):1027–1035, August 2006.

R. Leyva, A. Cid-Pastor, C. Alonso, I. Queinnec, S. Tarbouriech, and L. Martinez-Salamero1. Passivity-based integral control of a boost converter for large-signal stability. *IEE Proc - Control Theory and Applications*, 153(2):39–146, 2006.

Shengyi Liu and Roger Dougal. Dynamic multi-physics model for solar array. *IEEE Transactions on Industrial Electronics*, 17(2):285–294, June 2002.

C. Meza, D. Biel, J.Negroni, and F. Guinjoan. Boost-buck inverter variable structure control for grid-connected photovoltaic systems. In *International Symposium on Circuit and Systems*, 2005.

M. Prince. Silicon solar energy converters. *Journal of Applied Physics*, 26(5):534–540, May 1955.

W.J. Rugh. *Linear Systems Theory, 2nd Edition*. Pretice Hall, 1995.

Seth Sanders and George Verghese. Lyapunov-based control for switched power converters. *IEEE Transactions on Power Electronics*, 7(1):17–24, January 1992.

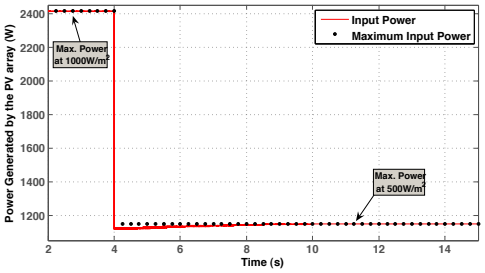

Fig. 10. P-Passive control simulation results: power generated by the PV array.

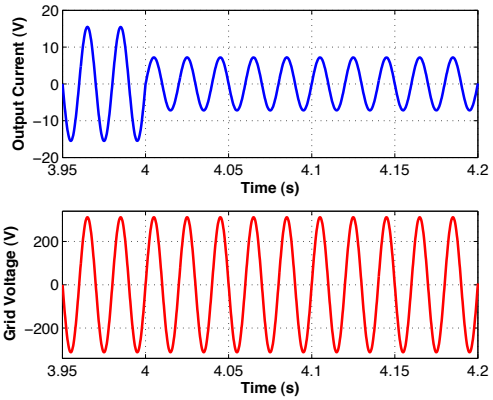

Fig. 11. P-Passive control simulation results: output current.

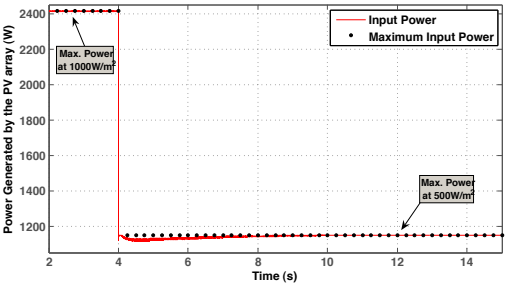

Fig. 12. P-Passive control + reference estimator simulation results: power generated by the PV array.

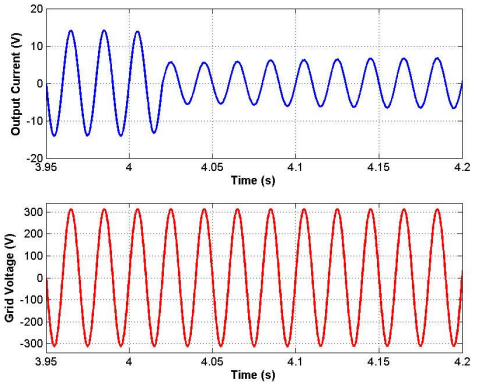

Fig. 13. P-Passive control + reference estimator simulation results: output current.